Published in final edited form as:
Cell. 2008 October 3; 135(1): 137–148. doi:10.1016/j.cell.2008.07.045.

ACF7 Regulates Cytoskeletal-Focal Adhesion Dynamics and Migration and Has ATPase Activity

Xiaoyang Wu[1], **Atsuko Kodama**[1,2], and **Elaine Fuchs**[1,*]
1*The Howard Hughes Medical Institute and Laboratory of Mammalian Cell Biology and Development, Rockefeller University, New York, NY 10065, USA*

Abstract

SUMMARY—Coordinated interactions between microtubule (MT) and actin cytoskeletons are involved in many polarized cellular processes. Spectraplakins are enormous (>500 kDa) proteins able to bind both MTs and actin filaments (F-actin) directly. To elucidate the physiological significance and functions of mammalian spectraplakin ACF7, we've conditionally targeted it in skin epidermis. Intriguingly, ACF7 deficiency compromises the targeting of microtubules along F-actin to focal adhesions (FAs), stabilizes FA-actin networks, and impairs epidermal migration. Exploring underlying mechanisms, we show that ACF7's binding domains for F-actin, MTs, and MT plus-end proteins are not sufficient to rescue the defects in FA-cytoskeletal dynamics and migration functions of *ACF7* null keratinocytes. We've uncovered an intrinsic actin-regulated ATPase domain in ACF7 and demonstrate that it is both functional and essential for these roles. Our findings provide insight into the functions of this important cytoskeletal crosslinking protein in regulating dynamic interactions between MTs and F-actin to sustain directional cell movement.

INTRODUCTION

Microtubules (MTs) and filamentous actin (F-actin) control diverse cellular functions, including cell shape, cell division, intra-cellular transport, adhesion, and movement. Increasing evidence suggests that intricate molecular interactions exist between these two seemingly distinct cytoskeletal networks (Goode et al., 2000; Palazzo and Gundersen, 2002; Rodriguez et al., 2003; Yarm et al., 2001). The coordination of cytoskeletal dynamics is particularly important for cell migration and adhesion, processes that are intrinsic and essential features of tissue morphogenesis and physiology.

The complex, multistep process of directed cell migration requires integrated activities of cytoskeleton, membrane, and cell/extracellular matrix (ECM) adhesions (Lauffenburger and Horwitz, 1996). Recent studies have pointed to an importance of MTs and coordinated MT/actin dynamics in cell migration (Palazzo and Gundersen, 2002; Rodriguez et al., 2003). It has long been known that MTs can be transported rearward in the lamellae of migrating cells, and this movement depends on actomyosin activity (Mikhailov and Gundersen, 1995; Waterman-Storer and Salmon, 1997; Yvon and Wadsworth, 2000). More recently, dual-wavelength fluorescent speckle microscopy has enabled visualization of MT coupling to retrograde actin flow in lamellae and also to anterograde actin movement within the cell body (Gupton et al.,

*Correspondence: E-mail: fuchslb@rockefeller.edu.
[2]Present address: Department of Dermatology, University of Texas Southwestern Medical Center, Dallas, TX 75390, USA

SUPPLEMENTAL DATA Supplemental Data include Supplemental Experimental Procedures, nine figures, and four movies and can be found with this article online at http://www.cell.com/cgi/content/full/135/1/137/DC1/.

2002; Salmon et al., 2002). Microtubules have also been shown to grow along F-actin bundles (Kodama et al., 2003).

One possible role for such coordinated actin-MT dynamics might be in mediating specific spatiotemporal regulation of FA dynamics to polarize cellular movements. Previous studies have demonstrated that MTs can specifically target peripheral FAs and promote their turnover, perhaps through MT motor-mediated delivery of key disassembly factors (Kaverina et al., 1998, 1999; Krylyshkina et al., 2002, 2003). Additional explorations reveal roles for FAK and dynamin in MT-induced FA turnover, suggestive of involvement of actin dynamics and endocytosis (Ezratty et al., 2005).

The molecular nature that underlies the potentially crucial coordination of MT-actin cytoskeletons at sites of focal adhesions in mammalian cells remains elusive, but accumulating evidence suggests that MT plus ends (+tips) and +tip-tracking proteins may mediate this cytoskeletal crosstalk (Akhmanova and Steinmetz, 2008; Carvalho et al., 2003; Wu et al., 2006). Although budding yeast lacks the major components of FAs, several tantalizing parallels exist between directed cell movement in mammalian cells and that which pulls and reorients the mitotic spindle along F-actin cables to its specific anchoring site within the yeast bud. In yeast, this intricate process requires an F-actin motor (Myo2) that binds to the adaptor protein Kar9, which in turn links indirectly to spindle MTs through the yeast homolog (Bim1) of the +tip protein EB1 (Kusch et al., 2003; Yarm et al., 2001).

Unique to multicellular organisms, spectraplakins are broadly expressed and are unusual in their ability to bind directly to and crosslink MT and F-actin networks (Jefferson et al., 2004; Leung et al., 1999; Sun et al., 2001; Yang et al., 1999). Genetic studies in lower eukaryotes suggest that their functions might be especially prominent in the epidermis and nervous system (Bosher et al., 2003; Jefferson et al., 2004; Roper et al., 2002). Of the mammalian spectraplakins, ACF7/MACF1 (actin crosslinking family 7/microtubule and actin crosslinking factor 1) is expressed and localized in patterns that most closely resemble *Drosophila* spectraplakin. Although preimplantation lethality precludes in vivo analysis, visceral endoderm cells derived from cultured *ACF7* null blastocysts reveal defects in the coordination of MT and actin cytoskeletons, accompanied by skewed cytoplasmic trajectories and altered dynamic instability of MTs. ACF7-deficient cells also fail to maintain cellular polarity in scratch-wounded cultures (Kodama et al., 2003).

In the present report, we employ conditional gene targeting to ablate ACF7 expression in skin of mice. Our findings have uncovered key roles for ACF7 in wound healing and epidermal migration, which we trace to an ability of ACF7 to target MTs that preferentially track along F-actin to FAs. By uncoupling this connection, we show that it is essential for controlling FA assembly and dynamics. Surprisingly, however, we find that the MT, F-actin, and +tip protein binding capabilities of ACF7 are not sufficient to rescue all of the functions of wild-type (WT) ACF7. Subsequently, we've identified an ~3000 residue central domain that bears sequence similarity to the Smc family of ATPases. We show that ACF7 can function as an ATPase, and, importantly, it behaves as an actin-regulated rather than MT- or calcium-regulated ATPase. Hitherto unrecognized in the spectraplakin family, this activity unveils important mechanistic insights into how spectraplakins evolved to function as unique macromolecular integrators that regulate dynamic actin-MT-mediated processes and how ACF7 in particular functions in establishing and maintaining proper cytoskeletal coordination during cell movement.

NIH-PA Author Manuscript

NIH-PA Author Manuscript

RESULTS

Conditional Targeting of ACF7 in the Epidermis

We conditionally targeted ACF7 by inserting two *loxP* sites flanking exon 6 and exon 7 (Figure S1 available online), which reside within the conserved plakin domain common to all known isoforms of ACF7 and other spectraplakins (Bernier et al., 2000; Jefferson et al., 2004; Karakesisoglou et al., 2000; Leung et al., 1999; Sun et al., 2001). Their deletion is predicted to shift the coding sequence of downstream exons. Mice homozygous for the germline floxed (flanking *loxP*) insertions were bred to *K14-Cre* recombinase transgenic mice, which efficiently excised floxed exons by embryonic day E15.5 (Vasioukhin et al., 1999) (Figure 1A). Neonatal mice genotypic for *K14-Cre* and $ACF7^{fl/fl}$ alleles (conditional knockout, cKO) were born in the expected Mendelian numbers and grew to normal size as adults. Immunoblot analyses with an antibody specific for all known ACF7 isoforms confirmed the reduction of protein in heterozygous animal skin epidermis (*K14-Cre:* $ACF7^{fl/+}$) and absence of ACF7 in cKO skin epidermis (Figure 1B). This was further verified by immunofluorescence, which documented the absence of ACF7 in epidermis and hair follicles (Figure 1C). Although the targeting could theoretically permit expression of a truncated N-terminal ACF7, immunoblot with an antibody recognizing the N-terminal sequence of ACF7 did not detect any low-molecular-weight protein product in KO keratinocyte lysate (Figure S2A), suggesting that the truncated protein was not expressed or unstable.

Conditional Acf7 Loss Results in Abnormalities in Wound Repair and Defects in Epidermal Cell Migration

Surprisingly, *ACF7* cKO animals showed no gross morphological changes in skin or hair coat. Histologically, epidermal homeostasis appeared normal, and immunofluorescence with antibodies against β4 integrin (basal surface of the epidermis), keratin 5 (basal layer), keratin 10 (spinous layer), and loricrin (granular layer) all displayed localization patterns analogous to WT skin (Figure S2B). However, when challenged to respond to injury, *ACF7* cKO skin exhibited a significant delay in repairing full-thickness wounds. Histological analysis and quantification revealed that the area of hyperproliferative epithelium (HE) that typically proliferates and migrates into the wound site was diminished by more than 30% over 2-4 days after injury. (Figures S2C and S2D, Figure 1D).

Interestingly, despite the delay in wound closure, no significant decrease was found in proliferation or apoptosis, as judged by labeling for phospho-histone H3, Ki67, or activated caspase 3, respectively (Figures S2D and S2E and data not shown). Rather, the delayed wound response in ACF7-deficient skin seemed more likely to be rooted in alterations in cell migration, which we documented by culturing primary keratinocytes (1°MK) from cKO and littermate control skins and monitoring the polarized rate of cell migration during recovery of ~500 μm scratches introduced into keratinocyte monolayers. Whereas WT 1°MK closed the gap within 36 hr, KO keratinocytes moved only ~20% of this distance into the gap (Figures 1E and 1F). As expected from our in vivo data, growth curve experiments showed no significant difference between KO and WT cells (Figure 1F).

Videomicroscopy permitted imaging and monitoring of the velocities and directed migration of individual keratinocytes. Assays of representative 1°MK highlighted the significantly slower movements of KO cells compared to their WT counterparts (Movie S1). Quantification of these movements revealed an ~60% decrease in average speed on fibronectin (FN) (Figures 1G and 1H). In contrast, when kymography was used to record membrane dynamics (Lauffenburger and Horwitz, 1996), no differences were detected in either duration of protrusion or protrusion rate (Figures S3A and S3B).

Cell Migration Defects Caused by ACF7 Deficiency Are Rooted in Perturbations in Epidermal-ECM Adhesion

To explore other possible mechanisms that might underlie ACF7 regulation of cell migration, we examined the contribution of cell/ECM adhesion to cell migration after ACF7 loss. To manipulate cell adhesive strength, we plated 1°MK onto dishes coated with FN at different concentrations (Gupton and Waterman-Storer, 2006; Palecek et al., 1997) and then recorded cell migration by videomicroscopy. Interestingly, by simply reducing the amount of underlying matrix protein, we were able to largely equalize the marked differences in velocities displayed by KO versus WT cells (Figure 2A). These data suggested that *ACF7* null 1°MK migrated aberrantly because they were defective in how they adhered to their underlying substratum.

Immunofluorescence microscopy revealed enhanced labeling of FAs in *ACF7* null 1°MK relative to WT controls (Figure 2B). Notably, the robust FAs in cells lacking ACF7 were also closely associated with cables of F-actin (stress fibers). Quantification documented a substantial increase in both size and total fluorescence intensity of FAs in KO 1°MK. Figure 2C shows the quantifications for vinculin, a representative structural component of FAs.

FA enlargement at the cell periphery is a sign of defects in FA dynamics, which are essential for cells to move (Berrier and Yamada, 2007; Burridge and Chrzanowska-Wodnicka, 1996; Delon and Brown, 2007; Lauffenburger and Horwitz, 1996; Ridley et al., 2003). To explore the nature of this defect in *ACF7* null 1°MK, we began by employing confocal videomicroscopy to trace the behavior of individual FAs (Webb et al., 2004). To monitor the process, we transfected cells with plasmids encoding either DsRed-Zyxin or GFP-Paxillin (Kodama et al., 2003; Schober et al., 2007).

Examples of the perturbations in FA dynamics arising from ACF7 deficiency are shown in complete form in Movie S2, and in montages are shown in Figure 3A. Most strikingly, in a 120 min interval of observation, FAs in KO cells were often static, whereas the majority of FAs in WT keratinocytes underwent continual bouts of formation, maturation, and disassembly. Quantifications of the kinetics of hundreds of individual FAs revealed a significant and marked decrease in both the assembly and disassembly rates of FAs in KO cells (Figure 3B). This was interesting, as FAK KO keratinocytes display defects in disassembly but not assembly rates (Schober et al., 2007).

The defects in FA dynamics were further substantiated by fluorescence recovery after photobleaching (FRAP) experiments (Figure 3C). By comparing GFP-Paxillin (Pxn)-transfected 1°MK, we found that ACF7 deficiency resulted in a strong decrease in the fraction of mobile protein and a significant increase in half-times of fluorescence recovery after bleaching (Figure 3D). Together, these data provide compelling evidence that FAs are more stable in the absence of ACF7, suggesting that ACF7 regulates cell migration at least in part by promoting FA dynamics.

Overall Activity of Rho GTPase and FAK/Src Signaling Are Unchanged in ACF7-Deficient Cells

Rho GTPases and their control of actomyosin activity are known to play a pivotal role in regulating FA dynamics and cell migration (Jaffe and Hall, 2005). However, biochemical pull-down assays revealed comparable overall levels of the GTP-bound state of RhoA, Rac1, and Cdc42 in WT and *ACF7* KO cells (Figures 3E and 3F). Similarly, no significant differences were detected in myosin light chain Ser19 phosphorylation, which correlates with myosin contraction activity (Figures S4A and S4B).

FA turnover typically involves a signaling pathway centering on FAK and Src tyrosine kinases, which are activated upon integrin-ECM engagement (Guan, 1997; Mitra et al., 2005).

NIH-PA Author Manuscript

NIH-PA Author Manuscript

However, *ACF7* null 1°MK exhibited no obvious change in either total FAK or Y397 phosphorylated (active) FAK (Guan, 1997; Parsons, 2003)(Figure 3G). Moreover, irrespective of ACF7 status, Y397 phosphorylation was abolished when cells were placed in suspension, suggesting that the dependency of activated integrins for FAK activity was not perturbed by loss of ACF7 function. Consistent with this notion, Src activity was unchanged as determined by phosphorylation levels of Y418 Src (Figure 3G). In suspension, WT and KO cells displayed similar decreases in Src activity. These findings were in good agreement with our kinetic studies and provided additional evidence that the impaired FA dynamics caused by ACF7 deficiency cannot be explained by alterations in the overall activity of Rho GTPases or FAK/Src signaling.

ACF7-Deficient Epidermal Keratinocytes Are Defective in Microtubule Targeting to Focal Adhesions

Given the absence of changes in Rho/FAK/Src activities in *ACF7*-null 1°MK and increasing evidence that MT targeting is involved in FA turnover (Kaverina et al., 1999; Rodriguez et al., 2003), we turned to the possibility that coordinated cytoskeletal dynamics and/or targeting of MT to FAs might be responsible for the defects in FA dynamics caused by loss-of-function mutations in ACF7. Interestingly, treatment of nocodazole, a MT-depolymerizing drug, dramatically reduced the rate of FA turnover in WT 1°MK to a similar level as in untreated KO cells. On the contrary, the same treatment did not further inhibit FA turnover in KO keratinocytes, despite their comparable sensitivity to the drug and comparable overall levels of polymerized tubulin (Figure 3H, Figure S5). These data suggested that ACF7's effect on FA disassembly in epidermal cells is mediated by polymerized MT networks.

Immunofluorescence microscopy unveiled additional defects in KO MT networks. In contrast to WT keratinocytes, where MTs bundles projected radially toward the cell periphery and paralleled the organization of actin stress fibers, MTs in *ACF7* null keratinocytes were often curled and bent and no longer coal-igned with actin cables (Figure 4A). Although the curly, bent behavior of MTs was remarkably similar to that observed in *ACF7* null endodermal cells (Kodama et al., 2003), the robust network of stress fibers and FAs in keratinocytes accentuated the extent to which coordination between actin and MT networks was disrupted in the absence of ACF7.

The prominent actin-FA network in keratinocytes led us to discover a striking and important perturbation in MT dynamics that had not been noted previously, namely that the MT ends that normally converge at peripheral FAs were missing in *ACF7* null cells (Figure 4B). Since ACF7 localized to these sites in WT keratinocytes (Figure 4B), we tested whether ACF7 might physically interact with +tip proteins, as has been found for two other spectraplakins (Kakapo and BPAG1) (Slep et al., 2005; Subramanian et al., 2003). As shown in Figure 4C, keratinocyte ACF7 specifically coimmunoprecipitated with +tip proteins EB1, Clasp1, and Clasp2, but not Clip170. Interestingly, however, the loss of ACF7 did not affect the ability of these proteins to localize to MT +tips (Figure S6). Taken together, our data suggested that ACF7 may mediate the interactions between MT +tips and actin-FA networks.

We directly tested this hypothesis by visualizing MT plus-end movements along F-actin bundles in the context of FAs. To do so, we had to simultaneously express GFP-EB1, DsRed-Zyxin, and CFP-actin in 1°MK and perform confocal videomicroscopy. Although MT plus ends are known to move along trajectories that coincide with stress fibers (Kodama et al., 2003; Krylyshkina et al., 2003; Salmon et al., 2002), triple fluorescence microscopy revealed that in keratinocytes, the MT plus-end movements along actin bundle tracks frequently terminated at FAs (Figure 4D, Movie S3). In marked contrast, the movement of EB1 ends in *ACF7* null 1°MK was random with respect to both actin cables and the targeting of MTs to FAs (Movie S3; quantification in Figure 4E). Facilitated by the multifluorescent probe strategy, this difference was particularly striking and provided compelling evidence that the gross alterations in coordination of MT and actin dynamics that occur upon ACF7 loss were manifested in a marked impairment in MT targeting to FAs. When coupled with our prior data on FA kinetics, the impairment in MT targeting in turn appeared to compromise FA turnover.

Microtubule-Actin Crosslinking Activity Is Not Sufficient for ACF7's Function in Cell Migration

Both static and dynamic structural interactions between MTs and F-actin have been documented or proposed in different systems (Rodriguez et al., 2003). A priori, static interactions could be mediated by individual proteins or protein complexes that associate with both cytoskeletal networks simultaneously, whereas dynamic interactions usually require a MT- or actin-based motor protein to drive relative movement between these two filaments.

To address how ACF7 mediates this process, we overcame the technical hurdles of its enormous size (5380 amino acid residues) and conducted mutagenesis and rescue experiments to identify the key domains involved. We first concentrated on the role of the MT- and F-actin-interacting domains. Immunoblot analyses revealed the bands expected from expressing GFP-tagged versions of full-length ACF7 as well as mutant proteins (ACF7-NC) consisting of the N-terminal F-actin binding domain (Karakesisoglou et al., 2000) and the C-terminal segment that harbors the putative +tip- and MT-interacting domains (Sun et al., 2001)(Figure 5A, Figure S7). Pull-down assays showed that both full-length ACF7 and ACF7-NC (81 kDa) associated with F-actin, MTs, and +tip proteins (Figures 5B and 5C).

We microinjected constructs to more precisely control concentration and ensure comparable expression of encoded proteins. Both ACF7 and ACF7-NC (but not GFP alone) restored overall MT organization and generated arrays of bundled filaments with radial trajectories (Figure 5D). However, ACF7-NC failed to rescue coordinated MT/actin dynamics in epidermal cells (Movie S4; Figure 5E). Thus, whereas EB1 accumulated on MT tips of ACF7-rescued cells, EB1 decorated MTs in ACF7-NC-expressing cells. Additionally, the MT bundles were much less dynamic when ACF7-NC rather than ACF7 was expressed.

Most importantly and in striking contrast to the WT, in ACF7-NC-expressing cells, EB1-decorated MTs frequently stopped at crosslinking sites with actin cables, and failed to display the fast actin-guided tracking to the periphery where robust FAs usually localized (Figure 5E). Additionally, only ACF7 restored the FA size and cell migration defects of KO 1°MK (Figures 5F and 5G). Collectively, these results unveiled an importance of ACF7 and coordinated dynamics of MT/actin in regulating FA turnover and cell migration. They also pointed to the view that to perform these functions, ACF7 must possess features that go beyond its ability to crosslink MT and actin networks and bind +tip proteins.

ACF7 Possesses an ATPase Activity

In ferreting out a possible explanation for why ACF7-NC restores overall MT-actin organization but not cytoskeletal dynamics, we searched for conserved sequence motifs within regions of ACF7 that were not present in ACF7-NC. Of note was an ~3000 amino acid residue stretch with considerable sequence similarity (e value: $3 \times e^{-20}$)to the Smc family of ATPases involved in chromosome segregation (Hirano, 2006). Two putative nucleotide binding motifs, Walker A and Walker B motifs (Hanson and Whiteheart, 2005), were also in this region (Figure S7). To ascertain whether ACF7 might possess intrinsic ATPase activity, we overexpressed ACF7-NC and HA-tagged ACF7 in cells and purified the proteins to more than 95% homogeneity (Figure 6A; Experimental Procedures).

To confirm that the recombinant proteins exhibited the expected F-actin and MT binding affinities, we conducted pull-down assays with either purified MTs or F-actin in vitro. With either ACF7-NC or HA-ACF7, a shift was observed from the supernatant to F-actin-bound or MT-bound fractions (Figure 6B). Pull-down and gel overlay assays also revealed a direct interaction between purified EB1 and ACF7 (Figure S8A). We were not able to show a similar direct association with either Clasp1 or Clasp2, suggesting that these interactions are indirect (Figure S8B). In this regard, it may be relevant that EB1 can form a complex with Clasp proteins (Mimori-Kiyosue et al., 2005). Whether EB1 functions as an adaptor to organize the +tip complex containing ACF7 and Clasp1/2 seems likely but is beyond the scope of the present study.

After validating the cytoskeletal interactions of ACF7 and ACF7-NC in vitro, we tested our purified recombinant proteins for ATP-hydrolysis activity. Autoradiography and quantification revealed significant ATP hydrolysis for full-length ACF7 in comparison to ACF7-NC or GST (Figure 6C). Interestingly, F-actin greatly enhanced the ACF7-dependent ATP hydrolysis, to a level comparable to that generated by equivalent picomolar amounts of myosin II. In contrast, F-actin alone had only negligible activity in hydrolyzing ATP, and it did not increase the baseline levels of ATP hydrolysis achieved by ACF7-NC (Figure 6C).

The ACF7- and F-actin-regulated ATPase activity did not appear to be attributable to myosin contamination, since a pan-myosin antibody able to detect 103 less myosin II protein than that used in the ATPase assays showed no reactivity with our purified ACF7 protein preparations (Figure 6D). Moreover, MTs showed no effect on ATP hydrolysis by ACF7 (Figure 6E). Additionally, although ACF7 contains two EF-hand motifs, its ATP-hydrolysis activity was not influenced by calcium (Figure 6F).

To further verify ACF7's ATPase activity and its function in cytoskeletal coordination and cell movement, we introduced a deletion mutation that removed the six-amino-acid Walker B (WB) motif (Figure S7) and used the same purification as we did for the WT to isolate ACF7-WB. With just these six residues missing out of the 5380 full-length protein, the mutant protein retained its ability to bind MTs and actin (Figures S9A and S9B) but was significantly compromised in actin-stimulated ATPase activity (Figure 6G). Moreover, when introduced into *ACF7* null 1°MK, ACF7-WB was less effective than ACF7 in reversing the FA and migration defects (Figure 6H). Taken together, these data suggest that the existence of an F-actin-responsive ATPase activity intrinsic to ACF7 provides a molecular explanation for ACF7's role in MT-actin dynamics and for why, in the absence of ACF7, FA turnover and cell migration are impaired.

DISCUSSION

Increasing evidence has pointed to essential roles for spectra-plakins in multicellular lower eukaryotes (Jefferson et al., 2004; Kodama et al., 2004). Despite this intrigue, the physiological significance of the closest mammalian homolog, ACF7, has remained unknown because of preimplantation lethality resulting from straight *ACF7* null mutations (Kodama et al., 2003). By employing conditional knockout technology, we've circumvented this problem, providing important insights into ACF7's roles in vivo. The importance of ACF7 in wound healing was not predicted from invertebrate studies. Our studies show that ACF7 is required for rapid and efficient formation of a hyperproliferative epithelium in response to injury and that its function is exerted primarily on epidermal migration rather than proliferation. Through a comprehensive approach encompassing biochemistry and molecular and cell biology, we further tackled the underlying mechanisms involved and unveiled a hitherto unrecognized role of ACF7 as an essential molecular goliath that integrates coordinated MT and actin dynamics, promotes MT targeting to FAs, and in turn enhances FA turnover and cell migration. This finding was particularly important because the molecular mechanisms that underlie MT targeting to FAs have been obscure.

FAs have long been known to associate with the actomyosin cytoskeleton, but it is only recently that they've emerged as the “hotspot” for crosstalk between MT and actin networks (Palazzo and Gundersen, 2002). In a series of elegant papers, Small's group has shown that MTs can specifically grow toward sites of FA, a process thought to be guided by underlying F-actin (Kaverina et al., 1998, 1999; Krylyshkina et al., 2002, 2003). These MT-targeting events temporally correlate with dissolution of FAs at the cell periphery, a feature in line with the long-standing observation that cells treated with MT-depolymerizing drugs display enlarged FAs (Bershadsky et al., 1996; Liu et al., 1998). Our study not only presents compelling genetic evidence in support of the hypothesis that targeting of MTs facilitates FA turnover, but it also illuminates ACF7 as a hitherto unappreciated and key player in this process.

Our data also provide important mechanistic insight into this process. Despite the defect in MT targeting and FA turnover, *ACF7* null cells have a rather normal actin cytoskeleton, actomyosin contractility appears unperturbed, and FAK/Src activities appear to be unaffected. Thus, it seems most likely that through the ability of ACF7 to target MTs to FAs, MTs serve as macromolecular tracks to deliver factors such as dynamin to facilitate FA turnover (Ezratty et al., 2005). The inability of nocodazole to exert any additive effect on the FA turnover rate abnormality in *ACF7* null cells lends further support to this notion.

Consistent with the sequence similarity (Slep et al., 2005) and prior studies with *Drosophila* Kapapo (Subramanian et al., 2003), we've shown that ACF7 not only has the ability to bind directly to F-actin and MTs, but also to MT +tip proteins, in this case, in a selective fashion. Like other +tip proteins (Akhmanova and Steinmetz, 2008; Carvalho et al., 2003; Wu et al., 2006), ACF7 regulates MT dynamic instability and mediates MT capture to cortical sites and/or F-actin (Kodama et al., 2003). A major new twist that developed from our studies is that AF7-NC, harboring the actin, MT and +tip binding domains, is not sufficient to rescue the defects in FA-cytoskeletal dynamics caused by loss of the full-length protein.

In discovering an actin-based ATPase activity for ACF7 and implicating it in this process, we've uncovered a mechanistic link between polarized actin-MT dynamics in budding-yeast cell division and mammalian cell migration that has long evaded the field. In budding yeast (Kusch et al., 2003; Yarm et al., 2001), Kar9 serves as a nodal point to organize a functional complex containing Bim1 (homolog of EB1) and a myosin V family actin motor protein, Myo 2, within the bud to mediate spindle orientation. APC (adenomatosis polyposis coli) and ACF7 have been postulated to be partial functional homologs of Kar9 owing to their EB1-binding capabilities (Fuchs and Yang, 1999; Rodriguez et al., 2003). However, Kar9 has no sequence homolog in multicellular organisms, and its ability to involve actin-based motor proteins has never found a eukaryotic counterpart. ACF7 now emerges as a higher eukaryotic protein that may be able to functionally and single-handedly replace the EB1-Kar9-Myo2 complex to mediate dynamic interactions between MTs and actin at specialized membrane sites, in this case FAs.

Future studies will be needed to fully understand how ACF7's newfound ATPase activity might be involved in coordinating the dynamics of MTs and F-actin. Fluorescence speckle microscopy has shown that different types of MT and actin interactions occur in migrating cells (Salmon et al., 2002). Many of these interactions are likely to be mediated by static crosslinking proteins. However, FA-associated actin stress fibers move away from FAs with a velocity of ~0.2-0.4 μm/min (Endlich et al., 2007; Hotulainen and Lappalainen, 2006), making it hard to visualize how the tracking behavior of MTs along actin stress fibers toward FAs could be mediated solely by static crosslinkers.

We favor the hypothesis that rather than physically moving MTs along F-actin, ACF7's ATPase activity might function in transporting the fast-moving +tip complex (0.15-0.4 μm/s) (Perez et al., 1999) along relative static actin stress fibers. This would ensure both the capping of fast-growing MT plus ends and the linkage of plus ends to the slowly moving actin networks. A schematic outlining this model is presented in Figure 7.

Consistent with this hypothesis, it is intriguing that ACF7-NC, which lacks the actin-responsive ATPase activity, failed to properly localize to the plus ends of microtubules, i.e., as expected for WT ACF7, nor was EB1 localization properly restored there. Also, the minigene did not rescue the defects in cytoskeletal and FA dynamics even though it harbored all of the known functional domains of spectaplakins (Movie S4). An inability of ACF7-NC to actively transport the +tip complex would explain why in the presence of this minigene, MT networks lacking ACF7 are transformed into an array of stable bundles with dramatically impaired dynamics of MTs along F-actin. Thus, although various models have been proposed to explain the plus-end enrichment of +tip proteins (Carvalho et al., 2003), our results suggest a new possibility, namely that ATPase activity associated with a protein such as ACF7 could maintain the essential +tip proteins at the plus ends of MTs during coordinated MT growth along F-actin to the FA. In closing, our findings add a fascinating new twist to the repertoire of spectraplakins' many diverse and critical functions and now pave the way for probing more deeply into their ability to orchestrate the crosstalk between actin and MT cytoskeletal networks and localized sites of membrane-associated activity.

EXPERIMENTAL PROCEDURES

Generation of ACF7 cKO Mice and Skin Wound Healing

The targeting vector was constructed so that exons 6 and 7 of *ACF7* gene were flanked by *loxP* sites (Figure S1). The linearized vector was transfected into mouse embryonic stem (ES) cells and homologous recombinant clones were identified by Southern blotting. *ACF7* cKO animals were generated by breeding of *ACF7*$^{fl/fl}$ mice to *K14-Cre* transgenic mice. All mice used in this study were bred and maintained at the Rockefeller University Laboratory Animal Research Center (LARC) in accordance with institutional guidelines.

For skin wound healing assays, same sex littermates of ~12-week-old mice were anesthetized, and two full-thickness 6 mm excisional wounds were made on both sides of the dorsal midline (Guasch et al., 2007). Mice were housed separately, and no self-induced trauma was observed in control or cKO mice. Tissue was collected 2-4 days after wounding, and wound re-epithelialization was evaluated by histological analyses. Hyperproliferative epidermis (HE) was identified by hematoxylin and eosin staining, and the length of HE that extended into the wounds was measured and quantified.

Cell Migration Assays, Time-Lapse Videomicroscopy, and Kymography

A scratch-wound healing assay was performed essentially as described (Wu et al., 2004). In brief, keratinocytes were plated on 35 mm tissue culture dishes coated with fibronectin. After cells reached confluency, wounds were created by manual scraping of the cell monolayer with a pipette tip. The dishes were then washed with PBS, replenished with media, and photographed with a phase-contrast microscope. Afterward, dishes were placed in the tissue-culture incubator, and the matched wound regions were photographed 12, 18, 24, 30, and 36 hr after wounding.

So that the movement of individual keratinocytes could be traced, cells were plated on fibronectin-coated dishes and imaged with an Olympus phase-contrast microscope (20×) for 3 hr at 2 frames/min and manually tracked in Metamorph (Universal Imaging). So that the membrane protrusive activity could be checked, cells were imaged with an Olympus phase-contrast microscope (40×) for 10 min at 20 frames/min. Metamorph was then used for the generation of kymography and analysis of the rate and duration of membrane protrusion.

FRAP and Focal Adhesion Assembly and Disassembly Measurements

Kinetics of FA assembly and disassembly were performed essentially as previously described (Schober et al., 2007; Webb et al., 2004). Keratinocytes were plated on fibronectin-coated dishes and transfected with plasmid encoding DsRed-Zyxin. Time series of images were acquired on a spinning-disc confocal microscope equipped with a 100× α-plane fluar (1.45 oil) lens and an EM charge-coupled device camera (Hamamatsu). The rate constants for focal adhesion assembly and disassembly were obtained by calculation of the slope of relative fluorescence intensity increases or decreases of individual focal adhesion on a semilogarithmic scale against time.

FRAP assays were performed essentially as described (Schober et al., 2007). In brief, cells were plated on fibronectin-coated 3.5 cm dishes and transfected with plasmid encoding GFP-paxillin. FRAP experiments were then performed on a microscope (DeltaVision; Stress Photonics) equipped with a 60× Plan APO N (1.42 oil) objective and immersion oil with refractive index of 1.514 (Applied Precision). Two or three prebleach events were performed, followed by a 1 s bleach event. Fluorescence recovery was recorded for 120 s after photobleaching events, and data from these photokinetic experiments were analyzed with DeltaVision software.

Preparation and Purification of Recombinant Proteins

GST or GST fusion proteins were produced and purified as described (Wu et al., 2004). pKH3S-ACF7 or pKH3S-ACF7-WB was transfected into 293F cells and selected by puromycin (5 μg/ml). Clone B8 was then adapted to suspension culture in serum-free medium and expanded. Crude lysates were collected in NP40 buffer (Wu et al., 2004) and purified by anti-HA affinity column. After being washed extensively with washing buffer (20 mM Tris-HCl, 1 M NaCl [pH 7.5]), proteins were eluted with elution buffer (20 mM Tris-HCl, 0.1 M NaCl, 0.1 mM ethylenediaminetetraacetic acid [EDTA, pH 7.5], 1 mg/ml HA peptide). Proteins were then separated by size-exclusion chromatography with Bio-Rad (Hercules, CA) Bio-Gel P100 column. Fractions were examined by SDS-PAGE, and fractions containing full-length ACF7 were combined and concentrated with Millipore Amicon Ultra (100K). Purified proteins were snap frozen in liquid nitrogen and kept at 80°C.

ATPase Assay

ATPase activity assays were performed as described (Kogan et al., 2002). In brief, purified proteins (2 pmol) were incubated with ATP and α-^{32}P-ATP in 10 μl of reaction buffer (15 mM Tris-HCl [pH 7.5], 25 mM KCl, 10 mM $MgCl_2$, 0.1 mM ethylene glycol tetraacetic acid [EGTA]). Purified tubulin and actin were polymerized in vitro (Cytoskeleton), and 1.5 μg of F-actin or MTs was used to check the influence of cytoskeleton on ATPase activity. In experiments where MTs were used, 0.2 μm of Taxol was included to stabilize MTs. To determine the effect of calcium, the reaction was carried out in reaction buffer supplemented with 1 mM $CaCl_2$. After incubation at 37°C for 1 hr, reactions were stopped by addition of 3.5 μl of stop buffer (10% SDS, 88% formic acid) and diluted 1:10 in water. One microliter of diluted reaction mixture was then spotted onto PEI-cellulose thin-layer chromatography (TLC) plates that were precleaned by ultra-pure water. TLC plates were developed in developing buffer (1 M Formic Acid, 0.5 M LiCl). Plates were air dried, and ATP hydrolysis was then visualized and quantified by autoradiography and densitometry. The ratio of ADP/ATP was used as an index for ATP hydrolysis.

Statistical Analysis

Statistical analysis was performed with Excel or OriginLab 7.5 software. Box plots are used to describe the entire population without assumptions on the statistical distribution. A Student's t test was used to assess the statistical significance (p value) of differences between two experimental conditions.

Supplementary Material

Refer to Web version on PubMed Central for supplementary material.

ACKNOWLEDGMENTS

We are grateful to Markus Schober, Mirna Perez-Moreno, Ellen Ezratty, and Michael Hack for discussion and helpful comments and to Ellen Wong, Maria Nikolova, June Racelis, Alison North, and Shivaprasad Bhuvanendran for their technical advice and assistance. We also thank William Earnshaw at University of Edinburgh for sharing reagents. The animal studies were performed with expert assistance from Lisa Polak and Nicole Stokes and were carried out in the Animal Lovers Against Animal Cruelty (ALAAC)-accredited LARC animal research facility at the Rockefeller University. This work was supported by a grant R01-AR27883 from the National Institutes of Health. E.F. is an investigator of the Howard Hughes Medical Institute. X.W. was an Anna D. Barker Fellow in Basic Cancer Research funded by the American Association for Cancer Research and is currently a postdoctoral fellow of the Jane Coffin Childs Memorial Fund for Medical Research.

REFERENCES

Akhmanova A, Steinmetz MO. Tracking the ends: A dynamic protein network controls the fate of microtubule tips. Nat. Rev. Mol. Cell Biol 2008;9:309–322. [PubMed: 18322465]

Bernier G, Pool M, Kilcup M, Alfoldi J, De Repentigny Y, Kothary R. Acf7 (MACF) is an actin and microtubule linker protein whose expression predominates in neural, muscle, and lung development. Dev. Dyn 2000;219:216–225. [PubMed: 11002341]

Berrier AL, Yamada KM. Cell-matrix adhesion. J. Cell. Physiol 2007;213:565–573. [PubMed: 17680633]

Bershadsky A, Chausovsky A, Becker E, Lyubimova A, Geiger B. Involvement of microtubules in the control of adhesion-dependent signal transduction. Curr. Biol 1996;6:1279–1289. [PubMed: 8939572]

Bosher JM, Hahn BS, Legouis R, Sookhareea S, Weimer RM, Gansmuller A, Chisholm AD, Rose AM, Bessereau JL, Labouesse M. The Caenorhabditis elegans vab-10 spectraplakin isoforms protect the epidermis against internal and external forces. J. Cell Biol 2003;161:757–768. [PubMed: 12756232]

Burridge K, Chrzanowska-Wodnicka M. Focal adhesions, contractility, and signaling. Annu. Rev. Cell Dev. Biol 1996;12:463–518. [PubMed: 8970735]

Carvalho P, Tirnauer JS, Pellman D. Surfing on microtubule ends. Trends Cell Biol 2003;13:229–237. [PubMed: 12742166]

Delon I, Brown NH. Integrins and the actin cytoskeleton. Curr. Opin. Cell Biol 2007;19:43–50. [PubMed: 17184985]

Endlich N, Otey CA, Kriz W, Endlich K. Movement of stress fibers away from focal adhesions identifies focal adhesions as sites of stress fiber assembly in stationary cells. Cell Motil. Cytoskeleton 2007;64:966–976. [PubMed: 17868136]

Ezratty EJ, Partridge MA, Gundersen GG. Microtubule-induced focal adhesion disassembly is mediated by dynamin and focal adhesion kinase. Nat. Cell Biol 2005;7:581–590. [PubMed: 15895076]

Fuchs E, Yang Y. Crossroads on cytoskeletal highways. Cell 1999;98:547–550. [PubMed: 10490093]

Goode BL, Drubin DG, Barnes G. Functional cooperation between the microtubule and actin cytoskeletons. Curr. Opin. Cell Biol 2000;12:63–71. [PubMed: 10679357]

Guan JL. Focal adhesion kinase in integrin signaling. Matrix Biol 1997;16:195–200. [PubMed: 9402009]

Guasch G, Schober M, Pasolli HA, Conn EB, Polak L, Fuchs E. Loss of TGFbeta signaling destabilizes homeostasis and promotes squamous cell carcinomas in stratified epithelia. Cancer Cell 2007;12:313–327. [PubMed: 17936557]

Gupton SL, Waterman-Storer CM. Spatiotemporal feedback between actomyosin and focal-adhesion systems optimizes rapid cell migration. Cell 2006;125:1361–1374. [PubMed: 16814721]

Gupton SL, Salmon WC, Waterman-Storer CM. Converging populations of f-actin promote breakage of associated microtubules to spatially regulate microtubule turnover in migrating cells. Curr. Biol 2002;12:1891–1899. [PubMed: 12445381]

Hanson PI, Whiteheart SW. AAA+ proteins: Have engine, will work. Nat. Rev. Mol. Cell Biol 2005;6:519–529. [PubMed: 16072036]

Hirano T. At the heart of the chromosome: SMC proteins in action. Nat. Rev. Mol. Cell Biol 2006;7:311–322. [PubMed: 16633335]

Hotulainen P, Lappalainen P. Stress fibers are generated by two distinct actin assembly mechanisms in motile cells. J. Cell Biol 2006;173:383–394. [PubMed: 16651381]

Jaffe AB, Hall A. Rho GTPases: Biochemistry and biology. Annu. Rev. Cell Dev. Biol 2005;21:247–269. [PubMed: 16212495]

Jefferson JJ, Leung CL, Liem RK. Plakins: Goliaths that link cell junctions and the cytoskeleton. Nat. Rev. Mol. Cell Biol 2004;5:542–553. [PubMed: 15232572]

Karakesisoglou I, Yang Y, Fuchs E. An epidermal plakin that integrates actin and microtubule networks at cellular junctions. J. Cell Biol 2000;149:195–208. [PubMed: 10747097]

Kaverina I, Rottner K, Small JV. Targeting, capture, and stabilization of microtubules at early focal adhesions. J. Cell Biol 1998;142:181–190. [PubMed: 9660872]

Kaverina I, Krylyshkina O, Small JV. Microtubule targeting of substrate contacts promotes their relaxation and dissociation. J. Cell Biol 1999;146:1033–1044. [PubMed: 10477757]

Kodama A, Karakesisoglou I, Wong E, Vaezi A, Fuchs E. ACF7: An essential integrator of microtubule dynamics. Cell 2003;115:343–354. [PubMed: 14636561]

Kodama A, Lechler T, Fuchs E. Coordinating cytoskeletal tracks to polarize cellular movements. J. Cell Biol 2004;167:203–207. [PubMed: 15504907]

Kogan I, Ramjeesingh M, Li C, Bear CE. Studies of the molecular basis for cystic fibrosis using purified reconstituted CFTR protein. Methods Mol. Med 2002;70:143–157. [PubMed: 11917519]

Krylyshkina O, Kaverina I, Kranewitter W, Steffen W, Alonso MC, Cross RA, Small JV. Modulation of substrate adhesion dynamics via microtubule targeting requires kinesin-1. J. Cell Biol 2002;156:349–359. [PubMed: 11807097]

Krylyshkina O, Anderson KI, Kaverina I, Upmann I, Manstein DJ, Small JV, Toomre DK. Nanometer targeting of microtubules to focal adhesions. J. Cell Biol 2003;161:853–859. [PubMed: 12782685]

Kusch J, Liakopoulos D, Barral Y. Spindle asymmetry: A compass for the cell. Trends Cell Biol 2003;13:562–569. [PubMed: 14573349]

Lauffenburger DA, Horwitz AF. Cell migration: A physically integrated molecular process. Cell 1996;84:359–369. [PubMed: 8608589]

Leung CL, Sun D, Zheng M, Knowles DR, Liem RK. Microtubule actin cross-linking factor (MACF): A hybrid of dystonin and dystrophin that can interact with the actin and microtubule cytoskeletons. J. Cell Biol 1999;147:1275–1286. [PubMed: 10601340]

Liu BP, Chrzanowska-Wodnicka M, Burridge K. Microtubule depolymerization induces stress fibers, focal adhesions, and DNA synthesis via the GTP-binding protein Rho. Cell Adhes. Commun 1998;5:249–255. [PubMed: 9762466]

Mikhailov AV, Gundersen GG. Centripetal transport of microtubules in motile cells. Cell Motil. Cytoskeleton 1995;32:173–186. [PubMed: 8581974]

Mimori-Kiyosue Y, Grigoriev I, Lansbergen G, Sasaki H, Matsui C, Severin F, Galjart N, Grosveld F, Vorobjev I, Tsukita S, Akhmanova A. CLASP1 and CLASP2 bind to EB1 and regulate microtubule plus-end dynamics at the cell cortex. J. Cell Biol 2005;168:141–153. [PubMed: 15631994]

Mitra SK, Hanson DA, Schlaepfer DD. Focal adhesion kinase: In command and control of cell motility. Nat. Rev. Mol. Cell Biol 2005;6:56–68. [PubMed: 15688067]

Palazzo AF, Gundersen GG. Microtubule-actin cross-talk at focal adhesions. Sci. STKE 2002;2002:PE31. [PubMed: 12096217]

Palecek SP, Loftus JC, Ginsberg MH, Lauffenburger DA, Horwitz AF. Integrin-ligand binding properties govern cell migration speed through cell-substratum adhesiveness. Nature 1997;385:537–540. [PubMed: 9020360]

Parsons JT. Focal adhesion kinase: The first ten years. J. Cell Sci 2003;116:1409–1416. [PubMed: 12640026]

Perez F, Diamantopoulos GS, Stalder R, Kreis TE. CLIP-170 highlights growing microtubule ends in vivo. Cell 1999;96:517–527. [PubMed: 10052454]

Ridley AJ, Schwartz MA, Burridge K, Firtel RA, Ginsberg MH, Borisy G, Parsons JT, Horwitz AR. Cell migration: Integrating signals from front to back. Science 2003;302:1704–1709. [PubMed: 14657486]

Rodriguez OC, Schaefer AW, Mandato CA, Forscher P, Bement WM, Waterman-Storer CM. Conserved microtubule-actin interactions in cell movement and morphogenesis. Nat. Cell Biol 2003;5:599–609. [PubMed: 12833063]

Roper K, Gregory SL, Brown NH. The `spectraplakins': Cytoskeletal giants with characteristics of both spectrin and plakin families. J. Cell Sci 2002;115:4215–4225. [PubMed: 12376554]

Salmon WC, Adams MC, Waterman-Storer CM. Dual-wavelength fluorescent speckle microscopy reveals coupling of microtubule and actin movements in migrating cells. J. Cell Biol 2002;158:31–37. [PubMed: 12105180]

Schober M, Raghavan S, Nikolova M, Polak L, Pasolli HA, Beggs HE, Reichardt LF, Fuchs E. Focal adhesion kinase modulates tension signaling to control actin and focal adhesion dynamics. J. Cell Biol 2007;176:667–680. [PubMed: 17325207]

Slep KC, Rogers SL, Elliott SL, Ohkura H, Kolodziej PA, Vale RD. Structural determinants for EB1-mediated recruitment of APC and spectraplakins to the microtubule plus end. J. Cell Biol 2005;168:587–598. [PubMed: 15699215]

Subramanian A, Prokop A, Yamamoto M, Sugimura K, Uemura T, Betschinger J, Knoblich JA, Volk T. Shortstop recruits EB1/APC1 and promotes microtubule assembly at the muscle-tendon junction. Curr. Biol 2003;13:1086–1095. [PubMed: 12842007]

Sun D, Leung CL, Liem RK. Characterization of the microtubule binding domain of microtubule actin crosslinking factor (MACF): Identification of a novel group of microtubule associated proteins. J. Cell Sci 2001;114:161–172. [PubMed: 11112700]

Vasioukhin V, Degenstein L, Wise B, Fuchs E. The magical touch: Genome targeting in epidermal stem cells induced by tamoxifen application to mouse skin. Proc. Natl. Acad. Sci. USA 1999;96:8551–8556. [PubMed: 10411913]

Waterman-Storer CM, Salmon ED. Actomyosin-based retrograde flow of microtubules in the lamella of migrating epithelial cells influences microtubule dynamic instability and turnover and is associated with microtubule breakage and treadmilling. J. Cell Biol 1997;139:417–434. [PubMed: 9334345]

Webb DJ, Donais K, Whitmore LA, Thomas SM, Turner CE, Parsons JT, Horwitz AF. FAK-Src signalling through paxillin, ERK and MLCK regulates adhesion disassembly. Nat. Cell Biol 2004;6:154–161. [PubMed: 14743221]

Wu X, Suetsugu S, Cooper LA, Takenawa T, Guan JL. Focal adhesion kinase regulation of N-WASP subcellular localization and function. J. Biol. Chem 2004;279:9565–9576. [PubMed: 14676198]

Wu X, Xiang X, Hammer JA 3rd. Motor proteins at the microtubule plus-end. Trends Cell Biol 2006;16:135–143. [PubMed: 16469495]

Yang Y, Bauer C, Strasser G, Wollman R, Julien JP, Fuchs E. Integrators of the cytoskeleton that stabilize microtubules. Cell 1999;98:229–238. [PubMed: 10428034]

Yarm F, Sagot I, Pellman D. The social life of actin and microtubules: Interaction versus cooperation. Curr. Opin. Microbiol 2001;4:696–702. [PubMed: 11731322]

Yvon AM, Wadsworth P. Region-specific microtubule transport in motile cells. J. Cell Biol 2000;151:1003–1012. [PubMed: 11086002]

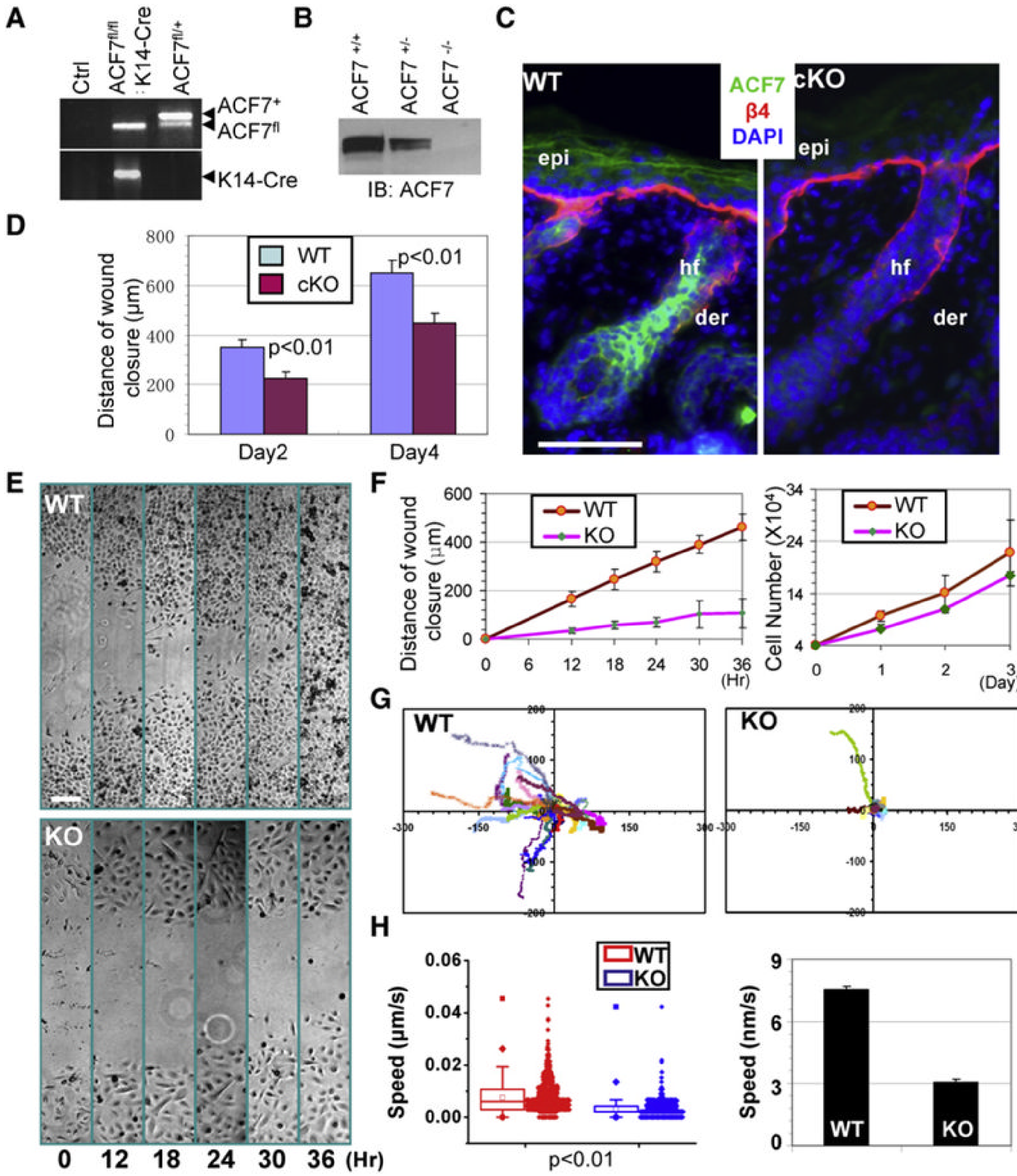

Figure 1. Conditional Targeting of ACF7 in Epidermis Results in Defective Wound Healing

(A) PCR genotyping of cKO mouse DNAs.

(B) Immunoblot (IB) analysis of P0 epidermal extracts probed with anti-ACF7 antibodies (Abs).

(C) Absence of ACF7 in epidermis (epi) and hair follicles (hf) of dorsal skin of targeted mice (cKO). Color coding is according to secondary Abs used in detection. Nuclei were counterstained with DAPI (blue). β4, β4-integrin; der, dermis.

(D) Quantification of the length of hyperproliferative epidermis (HE) generated at times indicated after wounding.

NIH-PA Author Manuscript
NIH-PA Author Manuscript

(E) Migration of confluent monolayers of 1°MK cultured from *ACF7* cKO and WT littermates and subjected to in vitro scratch-wound assays. Phase-contrast images of the site were taken at hours indicated after scratch wounding.
(F) Quantification of the kinetics of in vitro wound closure (left). Growth curves of the same cells are shown (right).
(G) Movements of individual 1°MK were traced by videomicroscopy. Migration tracks of 30 cells for each group (WT or KO) are shown here as scatter plots.
(H) Box and whisker plots of cell velocities indicating the mean (empty square within the box), 25th percentile (bottom line of the box), median (middle line of the box), 75th percentile (top line of the box), 5th and 95th percentiles (whiskers), 1st and 99th percentiles (solid diamonds), and minimum and maximum measurements (solid squares), with actual data points shown at right. The bar graph of cell velocities is shown (right). Error bars represent the SE.
The scale bars represent 50 μm.

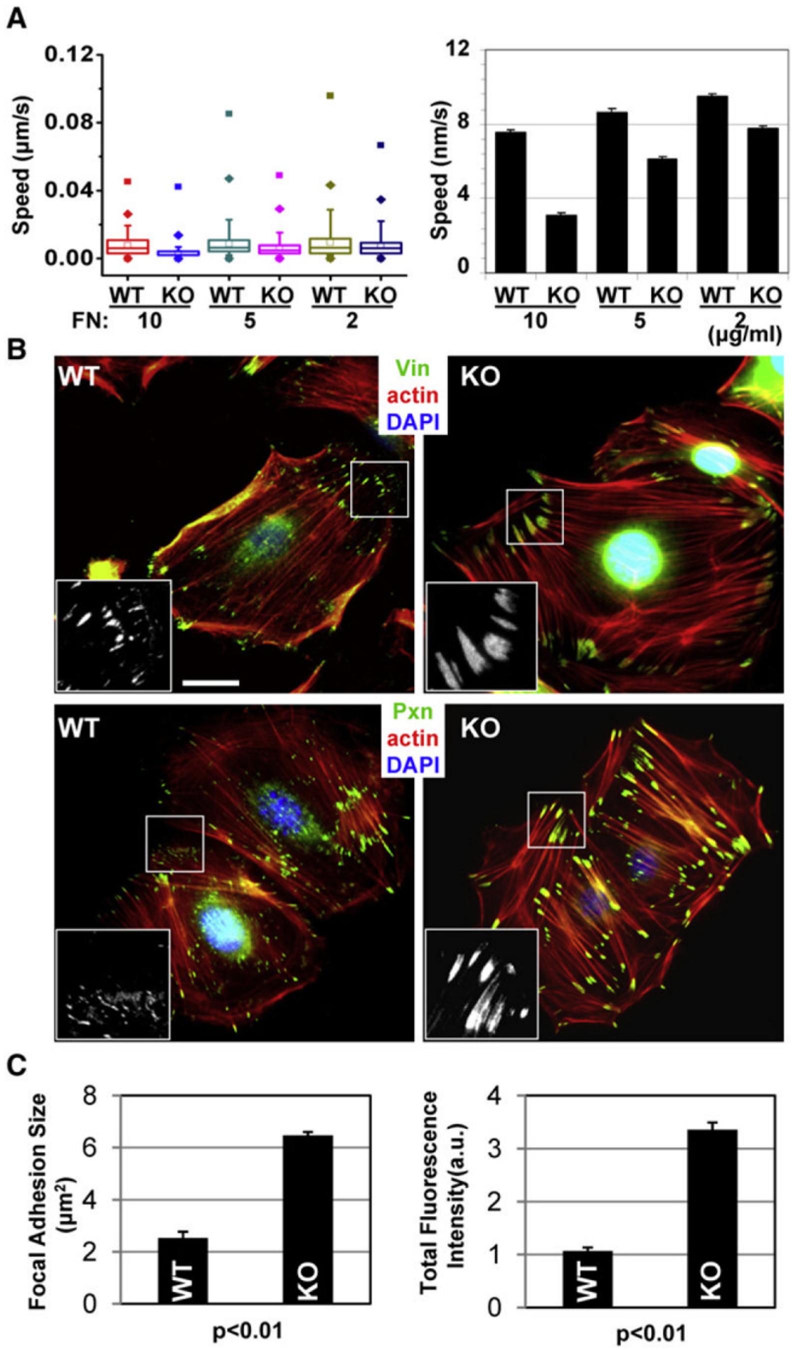

Figure 2. Cell Migration Defects in ACF7-Deficient 1°MK Are Rooted in Aberrantly Robust Focal Adhesions

(A) Box and whisker plots and bar graphs showing that migration velocities of WT and KO 1°MK are more equivalent at low fibronectin (FN) concentrations.

(B) Immunolabeling for F-actin (red), nuclei (DAPI; blue), and FA markers Vin and Pxn (green). Boxed areas are magnified in the insets, where only FA staining is shown. The scale bar represents 20 μm.

(C) Bar graphs indicating the size and total fluorescence staining intensity of FAs. Error bars of bar graphs represent the SE. a.u., arbitrary units.

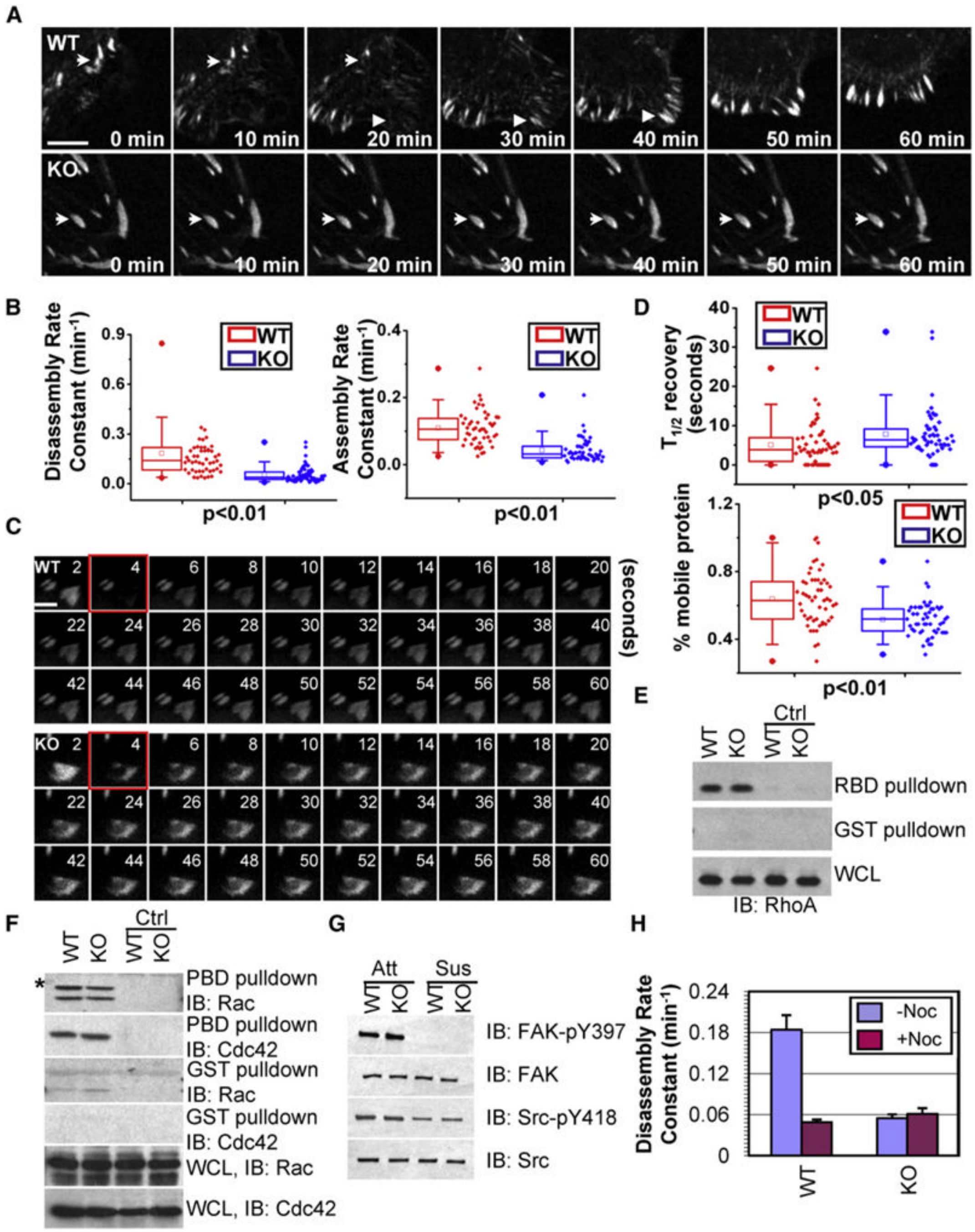

Figure 3. ACF7 Regulates FA Dynamics but Not by Altering Overall Rho GTPase and FAK/Src Activities

(A) Representative time-lapse images (montages) of DsRed-Zyxin-expressing 1°MK. Note the formation (arrowheads) and dissolution (arrows) of FAs in WT cells and very static FAs (arrows) in KO cells. The scale bar represents 5 μm.

(B) Box and whisker plots revealing slow assembly and disassembly rates of FAs in KO 1° MK relative to their WT counterparts.

(C) Fluorescence recovery after photobleaching (FRAP) (Schober et al., 2007) was used to visualize reduced dynamics of FAs in ACF7 KO versus WT cells expressing GFP-Pxn. Three prebleaching events were taken before 1 s (the fourth second) of photobleaching (highlighted by red frames), and fluorescence recovery was recorded for 120 s after photobleaching events. Representative time-lapse images of FAs are shown. The scale bar represents 2 μm.

(D) Box-and-whisker diagrams quantifying the differences in half-time ($T_{1/2}$) of FRAP and the mobile fraction of FA proteins between WT and KO cells.

(E and F) Activities of Rho, Rac, and Cdc42. Equal amounts of 1°MK proteins were either first loaded with GDP (served as negative control, ctrl) or directly incubated with GST or GST-PBD (PAK p21 binding domain) or GST-RBD (Rhotekin Rho binding domain) proteins bound to glutathione-coupled Sepharose beads to selectively pull down active Rac/Cdc42 or Rho. Bound proteins were washed and then subjected to SDS-PAGE followed by immunoblotting with different Abs as indicated. An aliquot of lysate was also analyzed (bottom panels) to ensure similar amount of protein inputs. * denotes nonspecific bands.

(G) FAK/Src activities. Aliquots of protein lysates from attached (Att) and suspended (Sus) 1°MK were analyzed by immunoblotting with the Abs indicated.

(H) Bar graphs revealing disassembly rates of FAs in 1°MK treated with or without nocodazole (13 μm).

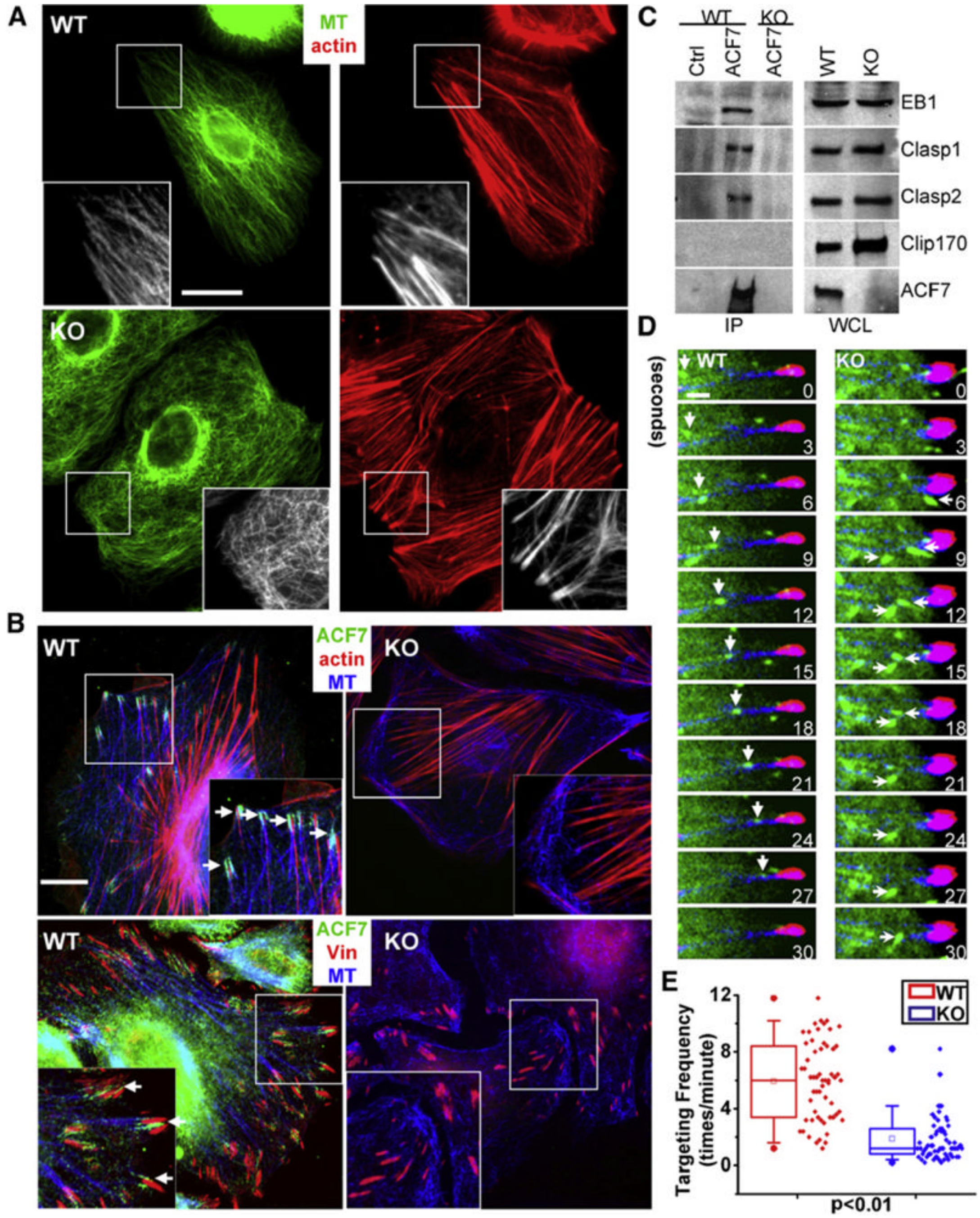

Figure 4. Loss of ACF7 Impairs Cytoskeletal Organization and the Ability of MTs to Target to Focal Adhesions

(A) Immunofluorescence for F-actin (red) and MTs (MT, β-tubulin staining, green) shows strikingly altered MT organization in KO versus WT 1°MK. The scale bar represents 20 mm. Boxed areas are magnified as insets.

(B) Coimmunostaining for ACF7 (green), MTs (blue), F-Actin, or vinculin (Vin, red) reveals that in WT cells, ACF7 localizes to the tips of MTs that are in close contact with F-actin cables and peripheral FAs, whereas in KO cells, MTs no longer target FAs. The scale bar represents 10 μm.

(C) ACF7 associates with selective +tip proteins. Equal amounts of 1°MK lysates were subjected to immunoprecipitation with Abs against ACF7 or control IgG. Immunoprecipitates (IP) and a control aliquot of whole-cell lysate (WCL) were analyzed by immunoblot with the Abs indicated.

(D) Representative time-lapse images of 1°MK expressing GFP-EB1, DsRed-zyxin, and CFP-actin to show MT plus-end growth (green) toward FAs (red) and tracking along underlying F-actin (blue). Note the EB1-decorated plus end of a MT (arrowheads) tracking along an actin stress fiber toward a FA in a WT cell. In contrast, directions of MT growth, marked by EB1 (arrows), are random in the absence of ACF7. The scale bar represents 1 mm.

(E) Behavior of MT targeting to FAs via F-actin was manually traced, and targeting frequencies to individual FAs were quantified and depicted by box-and-whisker diagrams. Note the dramatic alterations in the ability of MTs to track along actin fibers to FAs in the absence of ACF7.

NIH-PA Author Manuscript
NIH-PA Author Manuscript

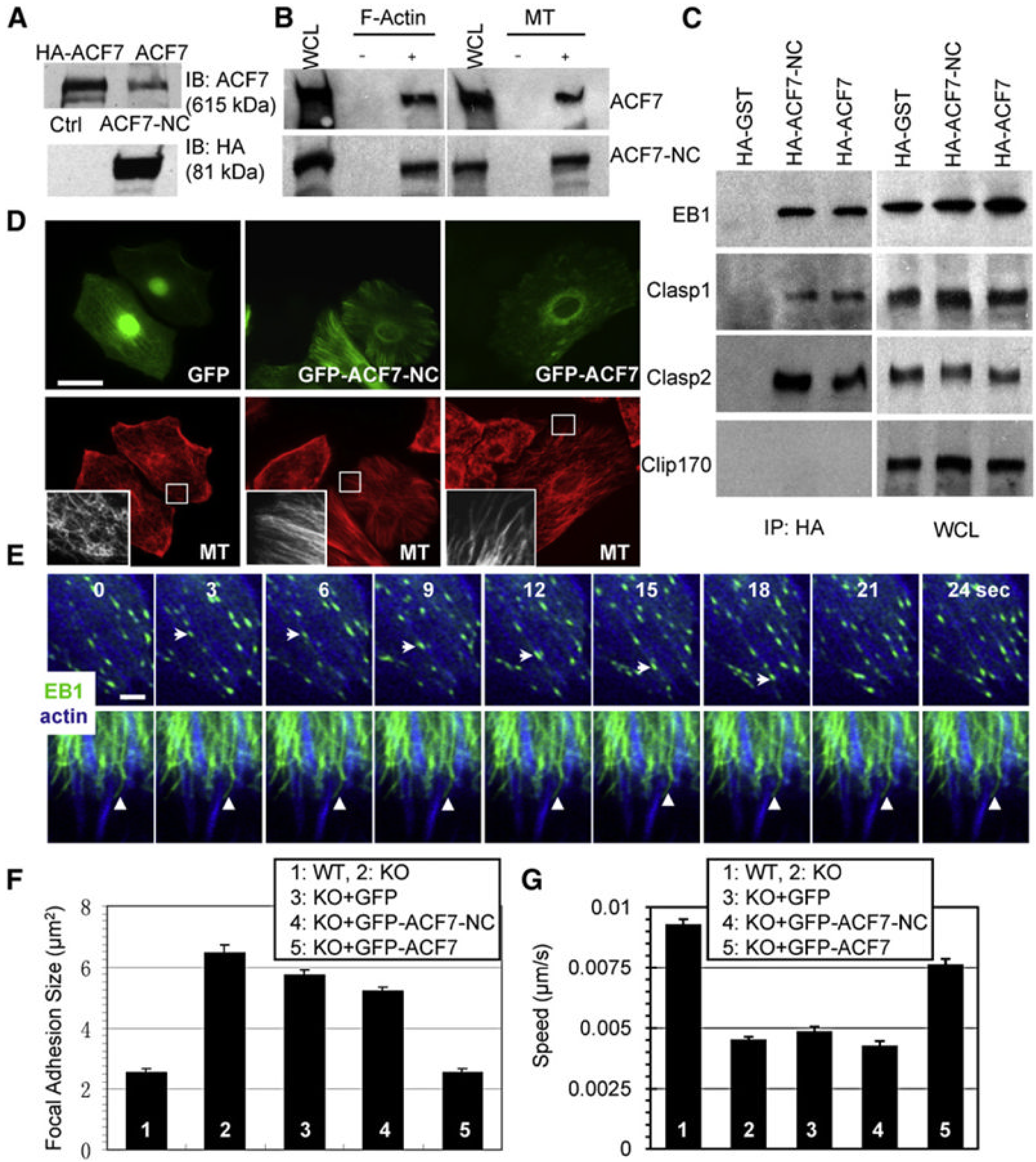

Figure 5. Microtubule/Actin Crosslinking and +tip Binding Activities Are Not Sufficient to Rescue the Defects in Keratinocyte Migration Caused by Loss of ACF7

(A) Lysates from cells ± full-length ACF7 (top panel) and lysates from cells ± ACF7-NC (bottom panel) were analyzed by immunoblots with the Abs indicated. Note that exogenously expressed ACF7 comigrates with the endogenous counterpart.

(B) Association of both full-length and ACF7-NC with F-actin and MTs. Lysates from cells transfected with HA-tagged full-length or ACF7-NC were incubated with purified F-actin or MTs, and cytoskeletal-bound and unbound proteins were separated by ultracentrifugation. Pellets were analyzed with a control aliquot of lysate by immuno-blot with HA Abs.

(C) Association of both full-length and ACF7-NC with +tip proteins. Lysates from cells transfected with HA-tagged full-length ACF7 or ACF7-NC or GST (control) were immunoprecipitated with HA Abs. Immunoprecipitates and a control aliquot of lysate were subjected to immunoblot assays with the Abs indicated.

(D) Rescue of MT organization defects by full-length and ACF7-NC proteins. KO cells injected with plasmids encoding GFP or GFP-ACF7-NC or GFP-ACF7 were immunostained for MT (β-tubulin staining, red). Boxed areas are magnified in the insets, where only MT staining is shown. The scale bar represents 20 μm.

(E) Failure of ACF7-NC to rescue F-actin-MT dynamics associated with FAs. Representative time-lapse images of full-length or ACF7-NC-injected KO keratinocytes expressing GFP-EB1 and CFP-actin to show MT plus ends (green) tracking along underlying F-actin (blue). Note the EB1 end (arrows) tracking along an actin stress fiber in the full-length ACF7-rescued cell. In ACF7-NC-expressing cells, EB1 decorated MTs instead of accumulating at plus ends. EB1-decorated MTs associated with underlying F-actin (arrowheads) but were excessively stable and failed to move along F-actin. The scale bar represents 2 μm.

(F and G) Quantifications of FA size and migration velocities for WT or KO 1°MK, or KO 1° MK injected with the plasmids indicated. Note that only full-length ACF7 restored FAs to their normal size and rescued the speed of migration. Error bars represent the SE.

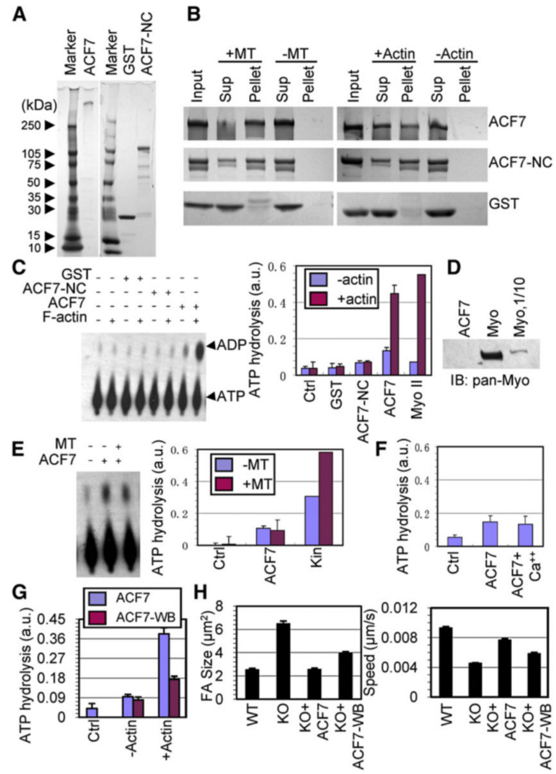

Figure 6. ACF7 Possesses an Actin-Responsive ATPase Activity

(A) Aliquots of purified recombinant ACF7 (calculated molecular mass 615 kDa), GST-ACF7-NC (106 kDa), and GST (27 kDa) were subjected to SDS-PAGE followed by silver-staining. Molecular mass markers in kDa are shown at left.

(B) Purified ACF7, ACF7-NC, and GST were incubated with or without micro-tubules (MT) or F-actin, and bound and unbound proteins were subsequently separated by ultracentrifugation. Pellets and supernatants (Sup) together with aliquots of input proteins were subjected to SDS-PAGE followed by staining with Coomassie blue.

(C) Representative autoradiography images of actin-regulated ATPase assays with the purified proteins (5 pmol) indicated. Bar graph at right shows quantifications of actin-regulated ATPase activities, along with equivalent picomolar amounts of myosin II (MyoII) as a control.

(D) Five or one-half (1/10) picomoles of purified myosin II and 5 pmol of purified ACF7 protein were analyzed by immunoblot assay with a pan-Myosin Ab.

(E) Representative autoradiography image of MT-dependent ATPase assay with the purified proteins indicated. Bar graphs indicate at right show quantifications of MT-dependent ATPase activities, along with equivalent picomolar amounts of CENPE kinesin motor domain as a control.

(F) Bar graph showing that the ATPase activity of ACF7 is not affected by calcium.

(G) Bar graph showing the decreased actin-stimulated ATPase activity of ACF7-WB (Walker B) deletion mutant compared with WT ACF7.

(H) Quantification of FA size and migration velocity for WT or KO 1°MK or KO 1°MK injected with the plasmids indicated. Note that ACF7-WB failed to restore the phenotype as effectively as WT ACF7. Error bars represent the SE.

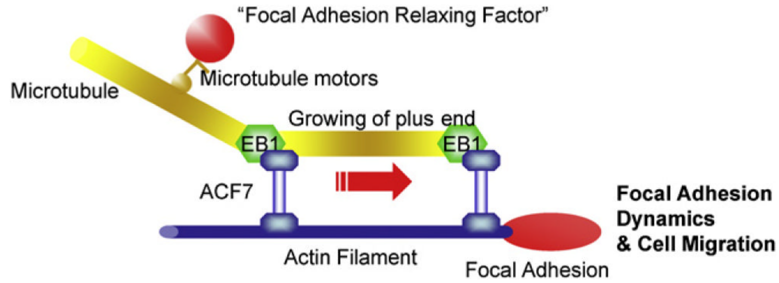

Figure 7. ACF7 Regulation of Cytoskeletal and Focal Adhesion Dynamics

A working model summarizing the role of ACF7 in cytoskeletal coordination and cell migration. We posit that ACF7's MT and F-actin binding activities together with its actin-regulated ATPase activity mediate the coordinated growth of MTs along F-actin, thereby guiding MTs to FAs. Targeted MTs at FAs may promote their dynamics and cell migration by serving as polarized tracks to deliver the "relaxing factors" via MT motor molecules.